Efficient continuous-wave self-Raman Yb:KGW laser with a shift of 89 cm^{-1}

M. T. Chang, W. Z. Zhuang, K. W. Su, Y. T. Yu, and Y. F. Chen*

Department of Electrophysics, National Chiao Tung University, Hsinchu 30010, Taiwan
**yfchen@cc.nctu.edu.tw*

Abstract: We demonstrated a continuous-wave (CW) self-Raman laser with high conversion efficiency by using Yb:KGW as the Raman crystal. The first Stokes line of wavelength centered at 1095.2 nm with spectral bandwidth of 8 nm and the cascaded Raman conversion wavelength at 1109.5 nm with spectral bandwidth of 3.4 nm were observed with a Raman shift of 89 cm^{-1} with respect to the fundamental laser wavelength at 1085.0 nm with spectral bandwidth of 10 nm. The CW Raman output power of 1.7 W was attained under the diode pump power of 7.8 W which corresponds to the slope efficiency and the diode-to-Stokes optical conversion efficiency of 26.6% and 21.8%, respectively.

OCIS codes: (140.3550) Lasers, Raman; (140.3580) Lasers, solid-state; (140.3615) Lasers, ytterbium.

References and links

1. A. A. Lagatsky, A. Abdolvand, and N. V. Kuleshov, "Passive Q switching and self-frequency Raman conversion in a diode-pumped Yb:KGd(WO_4)$_2$ laser," Opt. Lett. **25**(9), 616–618 (2000).
2. T. Omatsu, A. Lee, H. M. Pask, and J. Piper, "Passively Q-switched yellow laser formed by a self-Raman composite Nd:YVO_4/YVO_4 crystal," Appl. Phys. B **97**(4), 799–804 (2009).
3. Y. F. Chen, M. L. Ku, L. Y. Tsai, and Y. C. Chen, "Diode-pumped passively Q-switched picosecond Nd:$GD_xY_{1-x}VO_4$ self-stimulated raman laser," Opt. Lett. **29**(19), 2279–2281 (2004).
4. A. S. Grabtchikov, A. N. Kuzmin, V. A. Lisinetskii, V. A. Orlovich, G. I. Ryabtsev, and A. A. Demidovich, "All solid-state diode-pumped Raman laser with self-frequency conversion," Appl. Phys. Lett. **75**(24), 3742–3744 (1999).
5. A. A. Demidovich, A. S. Grabtchikov, V. A. Lisinetskii, V. N. Burakevich, V. A. Orlovich, and W. Kiefer, "Continuous-wave Raman generation in a diode-pumped Nd^{3+}:KGd(WO_4)$_2$ laser," Opt. Lett. **30**(13), 1701–1703 (2005).
6. H. Y. Zhu, Y. M. Duan, G. Zhang, C. H. Huang, Y. Wei, W. D. Chen, L. X. Huang, and Y. D. Huang, "Efficient continuous-wave YVO_4/Nd:YVO_4 Raman laser at 1176 nm," Appl. Phys. B **103**(3), 559–562 (2011).
7. V. N. Burakevich, V. A. Lisinetskii, A. S. Grabtchikov, A. A. Demidovich, V. A. Orlovich, and V. N. Matrosov, "Diode-pumped continuous-wave Nd:YVO_4 laser with self-frequency Raman conversion," Appl. Phys. B **86**(3), 511–514 (2007).
8. A. J. Lee, H. M. Pask, D. J. Spence, and J. A. Piper, "Efficient 5.3 W cw laser at 559 nm by intracavity frequency summation of fundamental and first-Stokes wavelengths in a self-Raman Nd:$GdVO_4$ laser," Opt. Lett. **35**(5), 682–684 (2010).
9. Y. Tan, X. H. Fu, P. Zhai, and X. H. Zhang, "An efficient cw laser at 560 nm by intracavity sum-frequency mixing in a self-Raman Nd:$LuVO_4$ laser," Laser Phys. **23**(4), 045806 (2013).
10. P. Dekker, H. M. Pask, D. J. Spence, and J. A. Piper, "Continuous-wave, intracavity doubled, self-Raman laser operation in Nd:$GdVO_{(4)}$ at 586.5 nm," Opt. Express **15**(11), 7038–7046 (2007).
11. L. Fan, Y. X. Fan, and H. T. Wang, "A compact efficient continuous-wave self-frequency Raman laser with a composite YVO_4/Nd:YVO_4/YVO_4 crystal," Appl. Phys. B **101**(3), 493–496 (2010).
12. V. A. Lisinetskii, A. S. Grabtchikov, A. A. Demidovich, V. N. Burakevich, V. A. Orlovich, and A. N. Titov, "Nd:KGW/KGW crystal: efficient medium for continuous-wave intracavity Raman generation," Appl. Phys. B **88**(4), 499–501 (2007).
13. P. Dekker, J. M. Dawes, P. A. Burns, H. M. Pask, J. A. Piper, and T. Omatsu, "Power scaling of cw diode-pumped Yb:KGW self-Raman laser," in *Proceedings of the Conference on Lasers and Electro-Optics Europe* (IEEE, 2003), pp. 50.
14. V. E. Kisel, V. G. Shcherbitsky, and N. V. Kuleshov, "Efficient self-frequency Raman conversion in a passively Q-switched diode-pumped Yb:KGd(WO_4)$_2$ laser," in Advanced Solid-State Photonics, J. Zayhowski, ed., Vol. 83 of *OSA Trends in Optics and Photonics* (Optical Society of America, 2003), paper 189.
15. A. Major, R. Cisek, and V. Barzda, "Development of diode-pumped high average power continuous-wave and ultrashort pulse Yb:KGW lasers for nonlinear microscopy," Proc. SPIE **6108**, 61080Y, 61080Y-8 (2006).

#196191 - $15.00 USD Received 21 Aug 2013; revised 21 Sep 2013; accepted 24 Sep 2013; published 7 Oct 2013

16. D. Kasprowicz, T. Runka, A. Majchrowski, and E. Michalski, "Low-temperature vibrational properties of $KGd(WO_4)_2$: (Er, Yb) single crystals studied by Raman spectroscopy," J. Phys. Chem. Solids **70**(9), 1242–1247 (2009).
17. J. Jakutis-Neto, J. Lin, N. U. Wetter, and H. Pask, "Continuous-wave watt-level Nd:YLF/KGW Raman laser operating at near-IR, yellow and lime-green wavelengths," Opt. Express **20**(9), 9841–9850 (2012).
18. D. C. Parrotta, W. Lubeigt, A. J. Kemp, D. Burns, M. D. Dawson, and J. E. Hastie, "Continuous-wave Raman laser pumped within a semiconductor disk laser cavity," Opt. Lett. **36**(7), 1083–1085 (2011).
19. Y. W. Wang, H. B. Cheng, Z. L. Zhu, J. L. Li, and J. H. Liu, "Structure and vibration spectrum of laser crystal $Yb:KGd(WO_4)_2$," J. Inorg. Mater. **20**(6), 1295–1300 (2005).
20. T. T. Basiev, A. A. Sobol, P. G. Zverev, L. I. Ivleva, V. V. Osiko, and R. C. Powell, "Raman spectroscopy of crystals for stimulated Raman scattering," Opt. Mater. **11**(4), 307–314 (1999).
21. H. Zellmer, S. Buteau, A. Tünnermann, and H. Welling, "All fibre laser system with 0.1 W output power in blue spectral range," Electron. Lett. **33**(16), 1383–1384 (1997).
22. E. B. Mejia, A. N. Starodumov, and Y. O. Barmenkov, "Blue and infrared up-conversion in Tm^{3+}-doped fluorozirconate fiber pumped at 1.06, 1.117 and 1.18 μm," Appl. Phys. Lett. **74**(11), 1540–1542 (1999).
23. F. Heinrichsdorff, Ch. Ribbat, M. Grundmann, and D. Bimberg, "High-power quantum-dot lasers at 1100 nm," Appl. Phys. Lett. **76**(5), 556–558 (2000).
24. S. D. Jackson, "2.7-W Ho^{3+}-doped silica fibre laser pumped at 1100 nm and operating at 2.1 μm," Appl. Phys. B **76**(7), 793–795 (2003).
25. Y. Tsang, B. Richards, D. Binks, J. Lousteau, and A. Jha, "A $Yb^{3+}/Tm^{3+}/Ho^{3+}$ triply-doped tellurite fibre laser," Opt. Express **16**(14), 10690–10695 (2008).
26. S. Uemura and K. Torizuka, "Kerr-lens mode-locking scheme for diode-pumped Yb-doped-bulk lasers," in Advanced Solid-State Photonics, OSA Technical Digest Series (CD) (Optical Society of America, 2008), paper MC36.
27. A. A. Lagatsky, N. V. Kuleshov, and V. P. Mikhailov, "Diode-pumped CW lasing of Yb:KYW and Yb:KGW," Opt. Commun. **165**(1–3), 71–75 (1999).
28. L. Fan, Y. X. Fan, Y. Q. Li, H. Zhang, Q. Wang, J. Wang, and H. T. Wang, "High-efficiency continuous-wave Raman conversion with a $BaWO_4$ Raman crystal," Opt. Lett. **34**(11), 1687–1689 (2009).
29. A. J. Lee, H. M. Pask, J. A. Piper, H. J. Zhang, and J. Y. Wang, "An intracavity, frequency-doubled $BaWO_4$ Raman laser generating multi-watt continuous-wave, yellow emission," Opt. Express **18**(6), 5984–5992 (2010).
30. H. Yu, Z. Li, A. J. Lee, J. Li, H. Zhang, J. Wang, H. M. Pask, J. A. Piper, and M. Jiang, "A continuous wave $SrMoO_4$ Raman laser," Opt. Lett. **36**(4), 579–581 (2011).
31. W. Lubeigt, V. G. Savitski, G. M. Bonner, S. L. Geoghegan, I. Friel, J. E. Hastie, M. D. Dawson, D. Burns, and A. J. Kemp, "1.6 W continuous-wave Raman laser using low-loss synthetic diamond," Opt. Express **19**(7), 6938–6944 (2011).
32. D. J. Spence, P. Dekker, and H. M. Pask, "Modeling of continuous wave intracavity Raman lasers," IEEE J. Sel. Top. Quantum Electron. **13**(3), 756–763 (2007).
33. J. Dong, K. Ueda, H. Yagi, A. A. Kaminskii, and Z. Cai, "Comparative study the effect of Yb concentrations on laser characteristics of Yb:YAG ceramics and crystals," Laser Phys. Lett. **6**(4), 282–289 (2009).
34. J. Dong, A. Shirakawa, K. I. Ueda, and A. A. Kaminskii, "Effect of ytterbium concentration on cw Yb:YAG microchip laser performance at ambient temperature - Part I: Experiments," Appl. Phys. B **89**(2–3), 359–365 (2007).
35. A. S. Grabtchikov, A. N. Kuzmin, V. A. Lisinetskii, G. I. Ryabtsev, V. A. Orlovich, and A. A. Demidovich, "Stimulated Raman scattering in Nd:KGW laser with diode pumping," J. Alloy. Comp. **300–301**(1–2), 300–302 (2000).
36. H. M. Pask, "Continuous-wave, all-solid-state, intracavity Raman laser," Opt. Lett. **30**(18), 2454–2456 (2005).
37. A. J. Lee, H. M. Pask, P. Dekker, and J. A. Piper, "High efficiency, multi-Watt CW yellow emission from an intracavity-doubled self-Raman laser using $Nd:GdVO_4$," Opt. Express **16**(26), 21958–21963 (2008).
38. T. Omatsu, M. Okida, A. Lee, and H. M. Pask, "Thermal lensing in a diode-end-pumped continuous-wave self-Raman Nd-doped $GdVO_4$ laser," Appl. Phys. B **108**(1), 73–79 (2012).
39. Y. M. Duan, H. Y. Zhu, G. Zhang, C. H. Huang, Y. Wei, C. Y. Tu, Z. J. Zhu, F. G. Yang, and Z. Y. You, "Efficient 559.6 nm light produced by sum-frequency generation of diode-end-pumped $Nd:YAG/SrWO_4$ Raman laser," Laser Phys. Lett. **7**(7), 491–494 (2010).

1. Introduction

Stimulated Raman scattering (SRS) in optical crystals has attracted great interest in recent years due to its extension of wavelength coverage in solid-state laser technologies. The pulsed-mode operations with high-peak-power were utilized in the past to reduce the restriction of high Raman threshold on solid-state Raman lasers [1–4]. Among solid-state Raman lasers, the self-Raman conversion that the laser crystal serves as the Raman medium simultaneously gains the advantages of compactness together with low resonator losses and thresholds. In 2005, the first continuous-wave (CW) Raman laser which utilized a Nd:KGW crystal as the self-Raman medium was demonstrated by Demidovich *et al.* [5]. Since then, various Nd-doped nonlinear crystals such as YVO_4 [6, 7], $GdVO_4$ [8], and $LuVO_4$ [9] have

#196191 - $15.00 USD Received 21 Aug 2013; revised 21 Sep 2013; accepted 24 Sep 2013; published 7 Oct 2013

been exploited to generate CW self-Raman lasers because of its wide applications in optical communications and biomedicine. However, the Raman conversion efficiencies of Nd-doped self-Raman media that range from 7.8% to 13.9% [6, 10–12] were hindered by low quantum efficiency and high thermal loading factor.

Yb-doped laser crystals have been proven to be promising materials for high efficiency owing to the small quantum defect, high quantum efficiency, and broad absorption bandwidth. Compared with other Yb-doped laser crystals, Yb:$KGd(WO_4)_2$ (Yb:KGW) crystal is a advantageous candidate for generating efficient self-Raman laser owing to its high absorption cross section (5.3×10^{-20} cm^2), large emission cross section (2.8×10^{-20} cm^2), and large nonlinear optical susceptibility $\chi^{(3)}$. Nevertheless, up to now, Yb:KGW self-Raman lasers were limited to the pulsed regimes in both actively Q-switched [13] and passively Q-switched [1, 14] operations.

The emission spectrum of the Yb:KGW crystal is shown in Fig. 1(a) which is re-plotted from [15]. Due to the quasi-three-level nature of the Yb:KGW crystal, the absorption and emission spectra are overlapping and the laser action can only be observed in the wavelength range from 1025 nm to 1090 nm [15] when the reabsorption loss is taken into consideration. The Raman spectrum of KGW as the Raman material measured by Kasprowicz *et al.* [16] is re-plotted in Fig. 1(b). Most of the previous works with KGW as the Raman material revealed that the mainly observed Raman shift lines were at 768 cm^{-1} [17, 18] and 901.5 cm^{-1} [12–14] owing to the large Raman gains. We can observe that, in addition to the strong Raman shift lines of 768 cm^{-1} and 901.5 cm^{-1}, there is still other Stokes shift for KGW host such as 89 cm^{-1}. This Stokes shift line is attributed to the strong translational mode of WO_4^{2-} ions [16] and has comparable or even larger Raman gain with respect to 768 cm^{-1} and 901.5 cm^{-1} [16, 19, 20]. Besides, the 89 cm^{-1} Stokes shift was experimentally observed as the cascaded Raman conversion of the first Stokes shift of 768 cm^{-1} [18]. With smaller Raman shift of 89 cm^{-1} in Yb:KGW crystal, laser wavelength near 1100 nm could be accessible which has a variety of applications, such as for fiber lasers emitting in the blue spectral range via upconversion [21–23] and Ho^{3+}-doped fiber laser to generate laser wavelength at 2.1 μm [24, 25].

In this work, we report, to the best of our knowledge, the first demonstration of CW self-Raman laser by Yb-doped crystalline material with high conversion efficiency. The first Stokes line of wavelength centered at 1095.2 nm with spectral bandwidth of 8 nm and the cascaded Raman conversion wavelength at 1109.5 nm with spectral bandwidth of 3.4 nm were observed with a Raman shift of 89 cm^{-1} with respect to the fundamental laser wavelength at 1085.0 nm with spectral bandwidth of 10 nm. Under the diode pump power of 7.8 W, the CW Raman output power of 1.7 W was attained by using a Yb:KGW crystal as the self-Raman medium. The corresponding slope efficiency and the diode-to-Stokes optical conversion efficiency was 26.6% and 21.8%, respectively.

2. Experimental setup

The schematic diagram of the experimental setup is depicted in Fig. 2. The diode-pumped, CW Yb:KGW self-Raman laser was composed of a plano-concave resonator. The gain medium was a 5 at.% doped Yb:KGW crystal with a length of 6 mm. Considering higher efficiency and more symmetric thermal lens, the gain medium was cut along the Ng-axis.

#196191 - $15.00 USD Received 21 Aug 2013; revised 21 Sep 2013; accepted 24 Sep 2013; published 7 Oct 2013

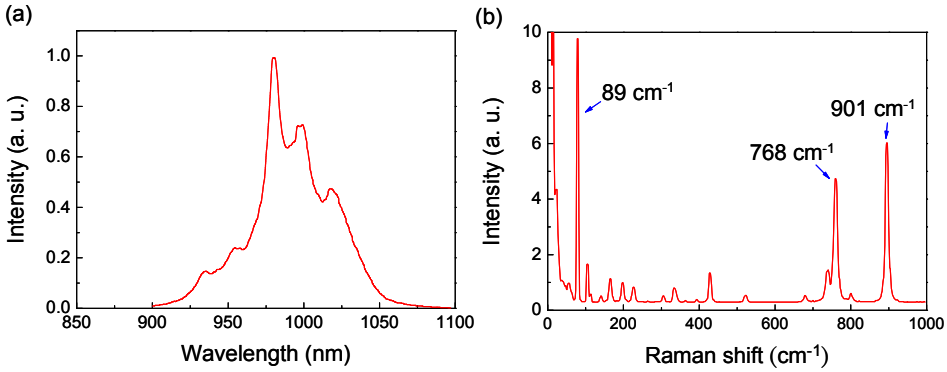

Fig. 1. (a) Fluorescence spectrum of Yb:KGW measured by Major et al. [15]. (b) Raman spectrum of $KGd(WO_4)_2$ measured by Kasprowicz et al. [16] for the $y(xx)z$ scattering geometry.

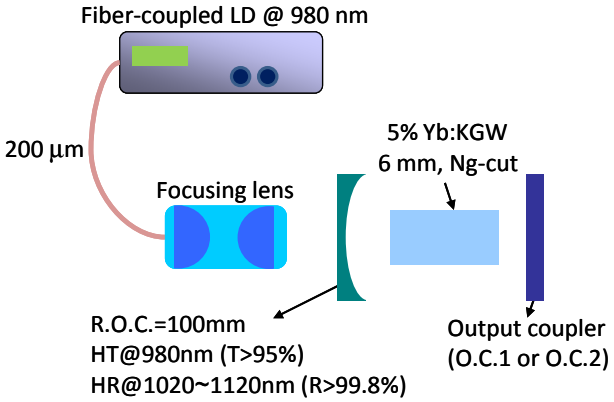

Fig. 2. Experimental setup for a CW diode-pumped Yb:KGW self-Raman laser.

Both the fundamental and self-Raman fields were found to be parallel to the Nm-axis. The present crystal cut was also suitable for achieving high gain on the 89 cm^{-1} Raman mode. Both sides of the active medium were coated for antireflection at 1000-1200 nm (R<0.2%). Additionally, the active medium was wrapped with indium foil and mounted in a water-cooled cooper block with water temperature to be maintained at 8 °C.

The input mirror is a concave mirror with the radius-of-curvature of 100 mm and coated with high-reflection (HR) coating at 1030-1120 nm (R>99.8%) together with high transmission (HT) coating at 980 nm (T>95%). Two flat output couplers (O. C.) with different coatings at both the fundamental laser range (from 1020 nm to 1090 nm) and the converted Raman laser range (from 1090 nm to 1110 nm) were used for comparison. The transmittance spectra of the O. C. were depicted in Fig. 3. The O.C.1 was designed to have higher reflection in both the fundamental laser range (R>99.8% from 1020 nm to 1090 nm) and in the converted Raman laser range (R>99.4% from 1090 nm to 1110 nm) than O.C.2 (R>99.5% @ 1020~1090 nm and R>99.0% @ 1090~1110 nm). The transmittance spectra were determined by a monochromator (Jobin-Yvon, Triax 320) which agree very well with the results specified by the manufacturer of the mirrors. Note that due to the low gain in CW Raman laser, all the coatings and optics setting should be designed to depress the cavity loss [6]. Besides, since the intracavity SRS efficiency is significantly sensitive to the cavity losses and thermal effects, the cavity length has to be as short as possible. Consequently, the

#196191 - $15.00 USD Received 21 Aug 2013; revised 21 Sep 2013; accepted 24 Sep 2013; published 7 Oct 2013

separation of the cavity mirrors was approximately 10 mm. The pumping source was a 980-nm fiber-coupled laser diode with a core diameter of 200 μm and a numerical aperture of 0.2. The focusing lens with 25 mm focal length and 90% coupling efficiency was used to focus the pump beam into the laser crystal. The pump spot radius was approximately 220 μm. The laser output spectral characteristics were investigated by an optical spectrum analyzer with 0.1 nm resolution (Advantest Q8381A).

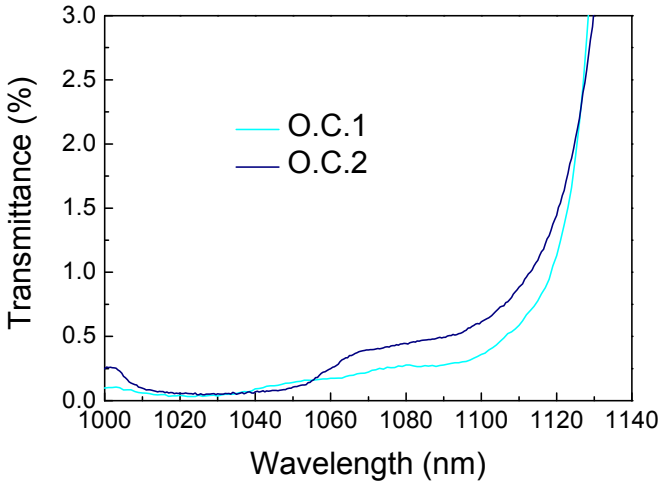

Fig. 3. The transmittance spectra of the used output coupler (O.C.1:output coupler 1; O.C.2:output coupler 2).

3. Experimental results and discussion

Figure 4 depicts the average total combined output power of the Stokes and fundamental wavelength with respect to the incident pump power of the laser diode. First, we use O.C.1 to demonstrate a CW self-Raman laser with high efficiency. The pump power threshold for the fundamental laser wavelength was 1.4 W. The maximum peak wavelength of the fundamental laser was located at 1088.9 nm with the total spectral bandwidth of 8.4 nm as demonstrated in Fig. 5(a). The present lasing wavelength was found to be considerably longer than the results ever reported [1, 13, 14] because the present cavity employed a relatively long gain medium and a fairly low output transmission for self-Raman generation. For a quasi-three-level medium, the lasing wavelength is determined by the resonator losses and the balance between emission and re-absorption. Since the re-absorption considerably reduces the short-wavelength net gain for low excitation levels, a cavity with a longer gain medium [26] or a lower output transmission [27] usually leads to a longer lasing wavelength [13]. By further increasing the pump power to 1.47 W, the intracavity fundamental field reached the threshold of the stimulated self-Raman generation with a shift of 89 cm^{-1}. As depicted in Fig. 5(b), the output spectrum near the Raman threshold displays simultaneously the fundamental and converted Raman components with a distribution ranging from 1080.0 nm to 1098.3 nm.

We observed that once the pump power got beyond the lasing threshold of the Raman conversion at 1.47 W, the lasing spectrum instantaneously stepped into the Stokes wavelength range which has the maximum wavelength peak centered at 1099.6nm as shown in Fig. 5(c). The output spectrum of the CW self-Raman laser under the maximum pump power of 7.8 W is shown in Fig. 5(d). Note that the fundamental optical field was nearly depleted due to high Raman conversion efficiency. Thus, the output spectra around the fundamental wavelength depicted in Figs. 5(c) and 5(d) need to be magnified by 1000 times for visibility. The integration time for the measurement of the optical spectrum is 10 seconds. The wide separation between longitudinal modes clearly shows that there is strong mode hoping and mode-competition between longitudinal modes. Even so, the instability of the average output

#196191 - $15.00 USD Received 21 Aug 2013; revised 21 Sep 2013; accepted 24 Sep 2013; published 7 Oct 2013

power is less than ± 2%. The first Stokes line that has maximum peak wavelength at 1099.6 nm and total spectral bandwidth of 12 nm was observed with a shift of 89 cm^{-1} with respect to the fundamental laser wavelength at 1088.9 nm. Above the threshold of the self-Raman generation, the Raman output power near 1095 nm increased linearly with increasing the pump power. The maximum Raman output power was as high as 1.7 W under the pump power of 7.8 W. The slope efficiency and the diode-to-Stokes optical conversion efficiency were found to be approximately 26.6% and 21.8%, respectively. Compared to the previous diode-to-Stokes optical conversion efficiency obtained in CW Raman lasers with self-Raman laser scheme (7.8% ~13.9%) [6, 10–12] and in separated-Raman laser operation (7.7% ~13.2%) [17, 28–31], the improvement of conversion efficiency is significant in the present result. Owing to the low gain in the CW Raman laser, the cavity losses and thermal effects usually lead to a substantial reduction on the conversion efficiency of the intracavity SRS. Here the Yb:KGW crystal was employed as the self-Raman medium with a smaller Raman shift of 89 cm^{-1}. This small Raman shift not only reduces the thermal effect due to smaller quantum defect but also increases the Raman gain coefficient. To the best of our knowledge, this is the highest diode-to-Stokes optical conversion efficiency attained with diode-pumped solid state lasers with CW Raman conversion. On the other hand, the fundamental output power near 1085 nm was found to be kept at a level of several mW for the pump power beyond the Raman threshold. The clamping of the fundamental output power agrees with the theoretical prediction that the intracavity power of the fundamental wave is almost fixed at its value at the Raman threshold for higher pump powers [32].

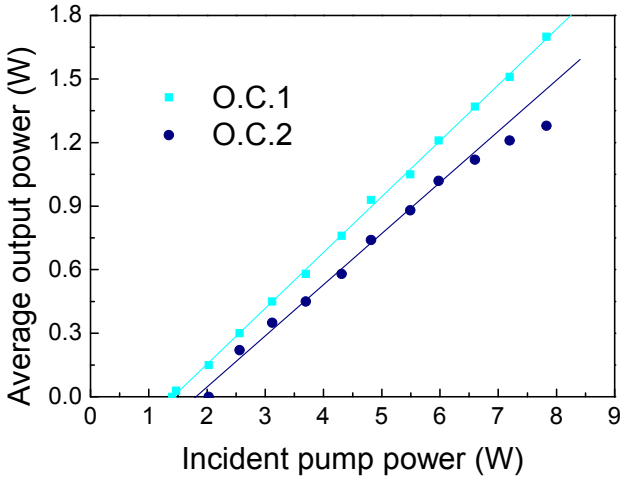

Fig. 4. The average total combined output power of the Stokes and fundamental wavelength with respect to the incident pump power by using different output coupler.

In order to confirm that the laser wavelength shift from 1088.9 nm to 1099.6 nm was resulted from the Raman conversion but not the wavelength shift induced by the re-absorption loss, we replaced the O. C. with O.C.2. The laser threshold with O.C.2 as the O.C. was 2.03 W and the output spectrum is depicted in Fig. 5(a') which centered at 1080.9 nm. The variant laser spectra with increased pump power were shown in Figs. 5(b')-5(d'). With the raised pump power from 2.03 W to 7.8 W, the center of the laser spectrum shifted gradually from 1080.9 nm to 1084.3 nm as depicted in Fig. 6. Since the spectral shape of the optical gain in a quasi-three-level medium significantly depends on the temperature, the red-shift with increasing the pump power is mainly caused by the temperature-dependent emission spectra of Yb-doped crystals [33, 34]. On the other hand, the output power exhibited the sign of rollover for the pump power higher than 7.0 W. The rollover was chiefly due to the gain degradation caused by the local heating.

#196191 - $15.00 USD Received 21 Aug 2013; revised 21 Sep 2013; accepted 24 Sep 2013; published 7 Oct 2013

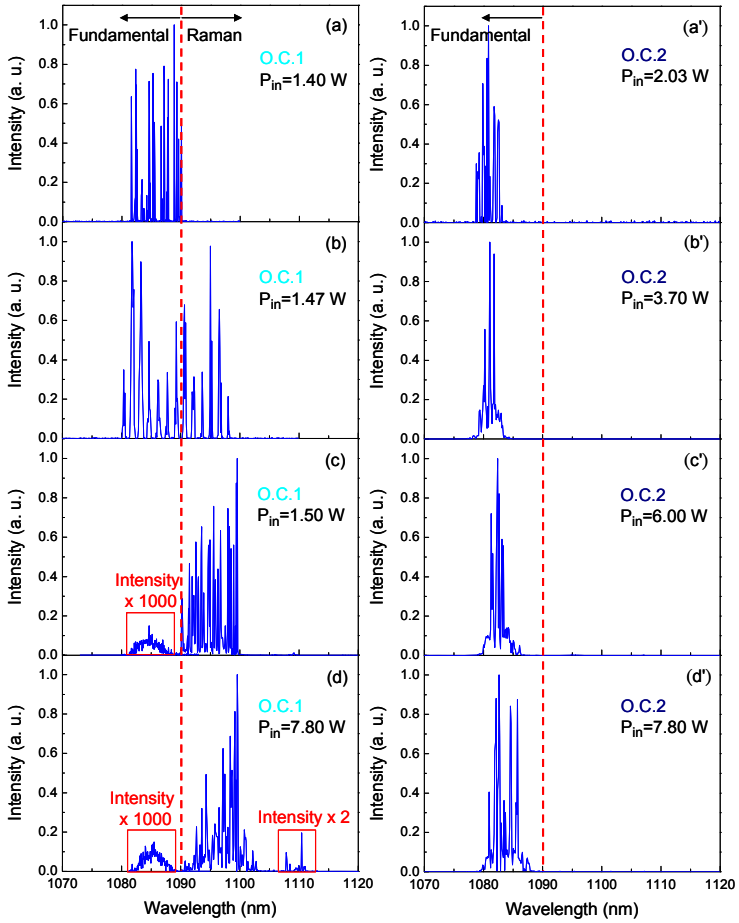

Fig. 5. (a)-(d) Laser output spectrum by using O.C.1 at various pump power of 1.40 W, 1.47 W, 1.50 W, and 7.80 W, respectively. Note: The intensities of the spectra of (c) together with (d) at around 1085 nm have been magnified by 1000 times and (d) at around 1110 nm has been magnified by 2 times. (a')-(d') Laser output spectrum by using O.C.2 at different pump power of 2.03 W, 3.70 W, 6.00 W, and 7.80 W, respectively.

In comparison with the result obtained with O.C.2, the case of using O.C.1 can be confirmed to come from Raman conversion by the following illustration. For the pump power just beyond the threshold of 1.47 W in the case with O.C.1, the wavelength of the maximum lasing peak suddenly shifted from 1088.9 nm to 1099.6 nm and nearly kept invariant with increasing the pump power. In contrast, the wavelength of the maximum lasing peak in the case of using O.C.2 gradually increased with increasing the pump power. The comparison is shown in Fig. 6. In the case of O.C.1, the abrupt jump of the lasing wavelength beyond the threshold of 1.47 W is an explicit indication for the generation of the Raman mode. Furthermore, as depicted in Fig. 5(d), a weak lasing output at 1110.5 nm could be detected. This wavelength component was just consistent with the second Stokes line, corresponding to the first Stokes line of 1099.6 nm with a further 89 cm^{-1} shift. All of the phenomena mentioned above certainly confirm that the wavelength shift obtained with O.C.1 was to come from the Raman conversion. Note that the reflectivities of the output coupler at 1188.3 nm and 1207.4 nm (which correspond to the Raman shift lines at 768 cm^{-1} and 901.5 cm^{-1} with the fundamental laser wavelength at 1088.9 nm) were 52.7% and 13.4%, respectively.

#196191 - $15.00 USD Received 21 Aug 2013; revised 21 Sep 2013; accepted 24 Sep 2013; published 7 Oct 2013

The reflectivities of the output coupler at these wavelengths were too low to depress the cavity loss for the low-gain CW Raman laser [6]. Thus, no Raman conversions at 1188.3 nm and 1207.4 nm were observed in this experiment.

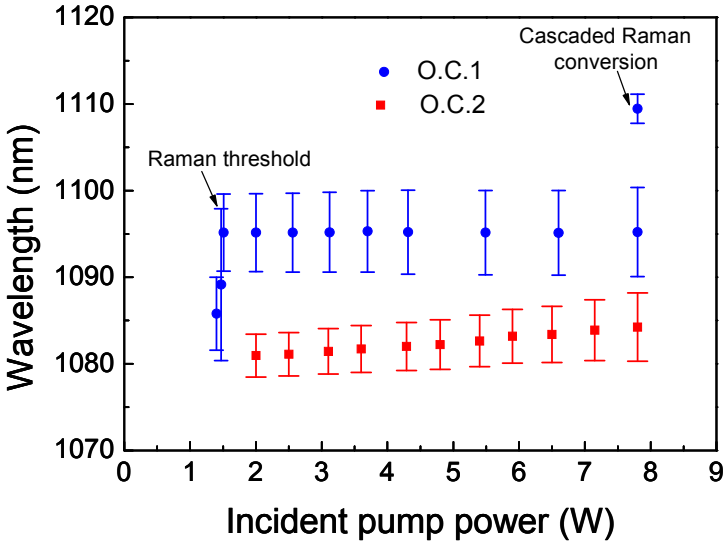

Fig. 6. Lasing wavelength versus various incident pump power with respect to different output coupler.

The diode pump power required to reach the Raman threshold can be simplified to be given by [32]

$$P_P = \frac{A_R}{g_R\, l_R}\frac{\lambda_F}{\lambda_P}\frac{(T_S + L_S)\,(T_R + L_R)}{2}, \qquad (1)$$

where A_R is the spot area of the Stokes field, g_R is the stimulated Raman gain coefficient, λ_P is the wavelength of the pump radiation, λ_F is the wavelength of the fundamental wave, T_F, L_F and T_S, L_S are the output coupling transmissions and round-trip losses for the fundamental and Stokes fields, respectively. With Eq. (1), the Raman threshold for the O.C.2 (T_F = 0.55%, T_S = 0.75%, L_F = 0.05%, L_S = 0.05%) can be estimated to be approximately 6 times higher than that for the O.C.1 (T_F = 0.2%, T_S = 0.3%, L_F = 0.05%, L_S = 0.05%). Using the experimental Raman threshold for the O.C.1, the pump power for the Raman generation with the O.C.2 needs to be higher than 8.0 W. Equation (1) also indicates that the Raman threshold can be reduced by decreasing the ration A_R / l_R through a combination of decreasing the mode size and increasing the crystal length. In addition, the Nd:KGW crystal can be expected to lead to a lower threshold for generating the 89 cm^{-1} Raman mode in comparison with the Yb:KGW crystal because it can offer a relatively higher Raman gain by a narrow bandwidth. Even so, the wide spectrum of the Yb:KGW laser can be employed to design the ultrafast mode-locked laser. It will be an interesting issue to achieve a self-Raman Yb:KGW laser in the mode locked operation.

When the Raman laser was under operation with O.C.1, a strong blue-red fluorescence within the space channel of laser generation from the Yb:KGW crystal can be observed by the naked eye and the emission spectrum measured by the optical spectrum analyzer was shown in Fig. 7. There were two spectral peaks shown in the spectrum which centered at 476.0 nm (blue fluorescence) and 649.1 nm (red fluorescence) with the spectral bandwidths of about 9 nm and 12 nm, respectively. The blue fluorescence phenomenon which has been previously observed by a variety of crystalline Raman laser materials such as KGW [35, 36], $GdVO_4$ [37, 38], $BaWO_4$ [28, 29], $SrWO_4$ [39], and $SrMoO_4$ [30] are characteristic of additional

#196191 - $15.00 USD Received 21 Aug 2013; revised 21 Sep 2013; accepted 24 Sep 2013; published 7 Oct 2013

energy deposition within the Raman crystal [29]. The up-conversion process within the Nd^{3+} ions for the case of Nd:KGW was speculated to be the origin of the blue luminescence [35]; while Pask *et al.* suggested that the blue fluorescence in the Raman crystals of un-doped KGW [36] and Nd:$GdVO_4$ [37] may be owing to trace impurity absorption by Tm^{3+} ions. Here we observed the blue-red luminescence in Yb-doped laser crystal under Raman generation. The origin of the blue-red luminescence within Yb:KGW crystal deserves further investigations.

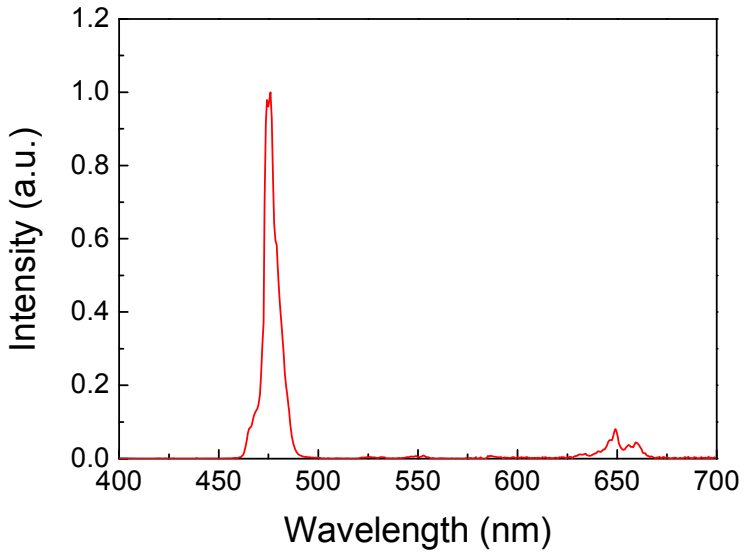

Fig. 7. Spectrum of the red-blue emission from the Yb:KGW crystal.

4. Conclusions

In conclusion, we have demonstrated, for the first time, a high efficiency Yb-doped CW self-Raman laser by using an Yb:KGW crystal. The CW Raman output power of 1.7 W was attained under the diode pump power of 7.8 W which corresponds to the slope efficiency and the diode-to-Stokes optical conversion efficiency of 26.6% and 21.8%, respectively. The first Stokes line of peak wavelength at 1099.6 nm and the cascaded Raman conversion wavelength at 1110.5 nm were observed with a Raman shift of 89 cm^{-1} with respect to the fundamental laser wavelength at 1088.9 nm. When the Raman laser was under operation, a strong blue-red fluorescence was detected at 476.0 nm and 649.1 nm, respectively.

Acknowledgments

The authors acknowledge the National Science Council of Taiwan for their financial support of this research under Contract NSC-100-2628-M-009-001-MY3.

#196191 - $15.00 USD Received 21 Aug 2013; revised 21 Sep 2013; accepted 24 Sep 2013; published 7 Oct 2013